J Solid State Electrochem (1998) 3: 31–38

ORIGINAL PAPER

Tomáš Grygar · Petr Bezdička

Electrochemical dissolution of Cr^{III} and Cr^{IV} oxides

Received: 20 February 1998 / Accepted: 31 March 1998

Abstract Oxidative dissolution of Cr oxides can be easily performed using voltammetry of immobilised microparticles. A combined procedure based on the dependence of current on time and potential (chronoamperometry with potential jumps) is suitable for the determination of the sensitivity of the dissolution rate to electrochemical potential. Applying this procedure, it was found that the rate determining step is preceded by two-electron oxidation in the solid phase that probably proceeds as a reversible equilibration between surface sites of Cr^{III}, Cr^{IV} and Cr^{V}. Voltammetry is sensitive to the phase composition, and so the voltammetric peak potentials obtained under the same conditions increase in the order $LaCrO_3 < CrO_2 < Me^{II}Cr_2O_4 < \alpha\text{-}Cr_2O_3$. The influence of Fe- and Ni-for-Fe substitution on dissolution reactivity is also discussed.

Key words Voltammetry · Cr oxides · Dissolution · Formal charge transfer coefficient

List of symbols

a	A constant value of formal charge transfer coefficient according to Eqs. 7, 10 and 16
a_L	An experimentally obtained, potential-dependent, local value of a defined by Eq. 9
$f(y)$	A geometrical contribution to the reactivity of microcrystalline solid (see [9] for details)
$k(E)$	A potential-dependent rate coefficient
k_{MAX}	Rate coefficient at a saturated reaction rate according to a surface complexation model [9]
y	A dimensionless fractional reaction, $y \in \langle 0, 1 \rangle$

T. Grygar (✉) · P. Bezdička
Institute of Inorganic Chemistry, Academy of Sciences,
CZ-250 68 Řež, Czech Republic
e-mail: grygar@uachr.iic.cas.cz

Introduction

Redox dissolution of Fe and Cr oxides is the fastest way to dissolve these otherwise chemically rather inert compounds [1, 2]. The topic is important in hydrometallurgy and nuclear technology, but it is also interesting from the theoretical point of view. Chemical oxidative dissolution of Cr_2O_3 and Fe,Cr mixed oxides in acids has already been studied [1], and particular attention has been paid to $KMnO_4$ [3] and $KBrO_3$ [4] as oxidants. According to Blesa et al. [1], the reaction with oxometallates proceeds via oxygen transfer from the oxidant to surface Cr^{III} sites and is mediated by the oxo bridge Cr—O—Me, i.e. by a formally two-electron reaction

$$\{\equiv Cr^{III}—O—Me\} \rightleftharpoons \{\equiv Cr^{V}\} + \text{products} \quad (1)$$

where $\{\equiv Cr^{n}\}$ denotes a surface site (hydrated and hydroxylated or protonated surface Cr ion).

A mechanism of chemical oxidative dissolution of Cr^{III} oxides by a chain of single-electron reactions with radicals has recently been proposed by Blesa et al. [1, 4, 5]. According to their scheme, dissolution is triggered by oxidation of $\{\equiv Cr^{III}\}$

$$\{\equiv Cr^{III}\} \rightleftharpoons \{\equiv Cr^{IV}\} + e^- \quad (2)$$

Although free Cr^{4+} ions are thermodynamically unstable and disproportionate to Cr^{3+} and Cr^{6+}

$$3Cr^{IV} \rightarrow 2Cr^{III} + CrO_4^{2-} \quad (3)$$

this valence state can be relatively stable in solid compounds. The primary oxidation product $\{\equiv Cr^{IV}\}$ can hence reach a certain steady-state concentration, e.g. it dominates on an $\alpha\text{-}Cr_2O_3$ surface in an oxidising solution at pH = 4 [5]. $\{\equiv Cr^{IV}\}$ is further oxidised to highly reactive $\{\equiv Cr^{V}\}$

$$\{\equiv Cr^{IV}\} \rightleftharpoons \{\equiv Cr^{V}\} + e^- \quad (4)$$

which is supposed to transform to a final soluble reaction product, CrO_4^{2-}. Pure Cr oxides dissolve fastest in

alkaline solution, but when another metal such as Fe is also present in the crystal lattice, dissolution in acids is preferred to avoid passivation of the reactant [1].

Because some Cr^{III} oxides are of medium to poor electronic conductivity, utilisation of the voltammetry of immobilised microparticles [6, 7] for the direct electrochemical study of their dissolution is available. The possibility of employing this simple and efficient method has already been demonstrated by electrochemical dissolution of Cr_2O_3 and CrO_2 [8, 9]. The theoretical basis for the electrochemical dissolution of microcrystalline metal oxides has been developed for Fe^{III} oxides [8–13]. As follows from the theory, all directly observable electrochemical characteristics of solid reactants are inherently affected by their phase composition, but also by their particle size and shape, the geometry of the movement of the reacting interface, and the individual properties of various solid samples (see particularly the reductive dissolution of α-FeOOH [13]). Such complexity may lead to certain scepticism towards unbiased result interpretation. We hence tried to separate the influence of potential on the reaction rate by an approach that has been employed in the kinetics of thermal reactions [14–16]. It is based on the determination of the sensitivity of a reaction rate to sudden changes of intensive variables. The main advantage of this "local" method is that no a priori kinetic modelling is required and that "sudden changes" can even be used for evaluating the correctness of this modelling [14].

The aim of this work was to compare the reactivity of several oxides containing Cr^{III} and/or Cr^{IV} constituents towards electrochemical oxidative dissolution. Particular attention was paid to the oxides with perovskite and spinel structures and to the influence of the Cr substitution. A method of potential jumps is proposed for the determination of the formal charge transfer coefficients and the results are compared with those based on simplified kinetic models. Our recent study revealed a significant sensitivity of electrochemical dissolution of α-FeOOH to Al- or Cr-for-Fe substitution [13], and hence we tested if the same is also true for substituted Cr oxides.

Experimental

The samples of Cr oxides used for electrochemical study are described in Table 1. Solid phase purity was checked by X-ray diffraction (XRD) (Siemens D-5005, Cu $K\alpha$ radiation). The synthetic routes were chosen to obtain well defined phases with fine crystals. The particle sizes were of the order of 10^{-1}–10^{-2} μm, which were checked by transmission electron microscopy (Phillips EM201, 80 kV).

The PC-controlled potentiostat μAutolab with GPES 4.4 software (Ecochemie Utrecht) was used for electrochemical measurements, with 0.1 M $HClO_4$/0.4 M $NaClO_4$ used as the supporting electrolyte. Voltammetry of immobilised Cr oxides was performed using a paraffin-impregnated graphite rod as the working electrode [8, 9, 13]. To prepare a carbon paste electroactive electrode, powdered spectral graphite was mixed with around 0.5 wt% of a solid sample and with the supporting electrolyte [18].

The potentiostatic procedure to obtain formal charge transfer coefficients α was described previously [8, 9, 13]. It is based on a series of measurements performed at varying potentials and the comparison of the resulting rate coefficients. Each potentiostatic curve is fitted to a function $f(y)$ that can be related to the consumption of the solid reactant [9]. $f(y)$ is a kinetic function describing the dependence of the rate of a heterogeneous reaction on the fractional reaction y

$$\frac{dy}{dt} = k(X_i) f(y) \tag{5}$$

where $k(X_i)$ is a rate coefficient at a given value of intensive variables X. This kinetic equation for a general heterogeneous reaction of microparticles can be adopted for an irreversible electrochemical reaction [8, 9, 12, 13]

$$\frac{I_t}{Q_0} = k(E) f\left(\frac{Q_t}{Q_0}\right) \tag{6}$$

where I_t is the actual current, Q_0 is the total charge of the electrode reaction and Q_t is the charge corresponding to the reactant remaining at time t. In this work, a potential range was chosen for potentiostatic measurements where $k(E)$ is a simple exponential function

$$k(E) = \exp\left(\frac{\alpha n F}{RT} E\right) = \exp(aE) \tag{7}$$

Equation 7 is valid only for low overpotentials, when the denominator in Eq. 10 is close to unity. The most generally applicable $f(y)$ for the voltammetry of microcrystalline oxides is the kinetic equation of a general reaction order

$$f(y) = \left(\frac{Q_t}{Q_0}\right)^{\gamma} \tag{8}$$

For more details see [9].

Table 1 The description of the solid samples studied

Crystal type	Cr valence	Sample	Synthetic route
Corrundum	III	α-Cr_2O_3	Heating $(NH_4)_2Cr_2O_7$ at 500 °C
Rutile	IV	CrO_2	Hydrothermal Synthesis [9]
Perovskite	III	$LaCrO_3$	Heating co-precipitated hydroxides at 1000 °C
	III	$La(Fe_xCr_{1-x})O_3$	Heating co-precipitated hydroxides at 1000 °C
	III + IV	$La(Co_{0.5}Cr_{0.5})O_3$	Heating co-precipitated hydroxides at 1000 °C
	III + IV	$La(Ni_xCr_{1-x})O_3$	Heating co-precipitated hydroxides at 1000 °C
Spinels	III	$ZnCr_2O_4$	Drying solution of $ZnCl_2$ and $(NH_4)_2Cr_2O_7$ and heating the residue
	III	$NiCr_2O_4$	Grinding NiO and Fe_2O_3 and heating at 1000 °C
	III	$FeCr_2O_4$	Heating Fe, Fe_2O_3, and Cr_2O_3 at 1000 °C in vacuum
	III	$Co(Fe_xCr_{1-x})_2O_4$	Heating co-precipitated hydroxides at 1000 °C
	III	$Ni(Fe_xCr_{1-x})_2O_4$	Heating co-precipitated hydroxides at 1000 °C
	III	$Zn(Fe_xCr_{1-x})_2O_4$	Heating co-precipitated hydroxides at 1000 °C

Results

All synthesised Cr oxides are electrochemically oxidisable in acidic solution. If the scan rate is of the order of mV s^{-1} or lower, the reaction is complete within a single voltammetric measurement. To demonstrate the chemical nature of the process, $LaNi_{0.15}Cr_{0.85}O_3$ was added to a carbon paste and cyclic voltammetry was performed (see Fig. 1). The first significant electrochemical reaction of a fresh electrode is solid-phase oxidation. It is followed by reduction of the formed CrO_4^{2-} in the subsequent cathodic scan. To identify the species responsible for the latter peak, the carbon paste electrode with dissolved dichromate (0.03 M) was used (see a procedure to distinguish solid and soluble reactants in carbon paste electroactive electrodes [18]). Cr^{3+} so created is probably not oxidised at potentials that are sufficient for dissolution of the studied Cr oxides. This is in accordance with the fact that chemical oxidative dissolution of $\{\equiv Cr^{III}\}$ is much faster than that of dissolved $Cr^{3+}(aq)$ under the same conditions [4].

In contrast to the carbon paste method, the only process which can be observed using voltammetry of immobilised $LaNi_{0.15}Cr_{0.85}O_3$ is the oxidation of the solid. Comparing both voltammetric methods, it is easy to distinguish the reactions of soluble and solid species. The simplicity of the voltammetric spectrum without any interference caused by the soluble reaction products made us prefer the voltammetry of immobilised solid particles to the carbon paste electroactive electrode. As for the critics of the appearance of voltammetric peaks obtained by the former method [19], one must keep in mind that the irreversible processes of solids can yield wider and possibly less symmetric peaks than are those of reversible or quasi-reversible reactions of soluble ions. The peak shape also mirrors the inherent characteristics of the solid reactants, such as granulometric properties and the "individuality" of each sample.

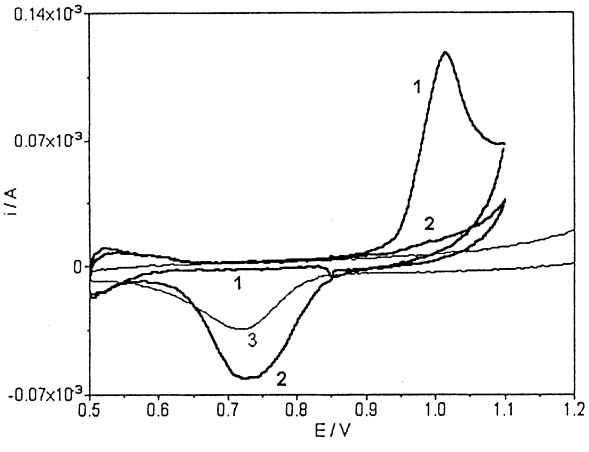

Fig. 1 Voltammograms of carbon paste electroactive electrodes. *1*, *2* $LaCr_{0.85}Ni_{0.15}O_3$, *3* 0.03 M dichromate. First scan from 0.85 V towards negative potentials

The principle of the proposed potential-jump method is shown in Fig. 2. It is based on performing a chronoamperometric experiment at potential E_B for a time t_B, then at potential $E_B+\Delta$ for t_Δ that is sufficiently long to obtain a pure Faradaic current $I_{B+\Delta}$ but sufficiently short to dissolve as small a fraction of the solid as possible, and then the experiment continues at E_B for a sufficiently long time to estimate the hypothetical value of the current I_B during the potential pulse between t_B and $t_B+ t_\Delta$ that could be expected at E_B. That potential programme can be easily performed with the utilised software (see Experimental). Typical values used for the potential-jumps were $t_B = 30$–200 s, $\Delta = 0.01$ or 0.02 V and $t_\Delta = 8$–30 s. The local values of a formal charge transfer coefficient can be obtained from Eq. 9

$$a_L = \frac{nF}{RT}\alpha_L = \frac{\ln(I_{B+\Delta}) - \ln(I_B)}{\Delta} \tag{9}$$

The subscript L denotes a local value which is a function of applied potential. Note that a is a calculated constat in Eqs. 7, 10 and 16 whereas a_L is a more directly obtained function. The current reached its steady-state value within less than a few seconds after applying the

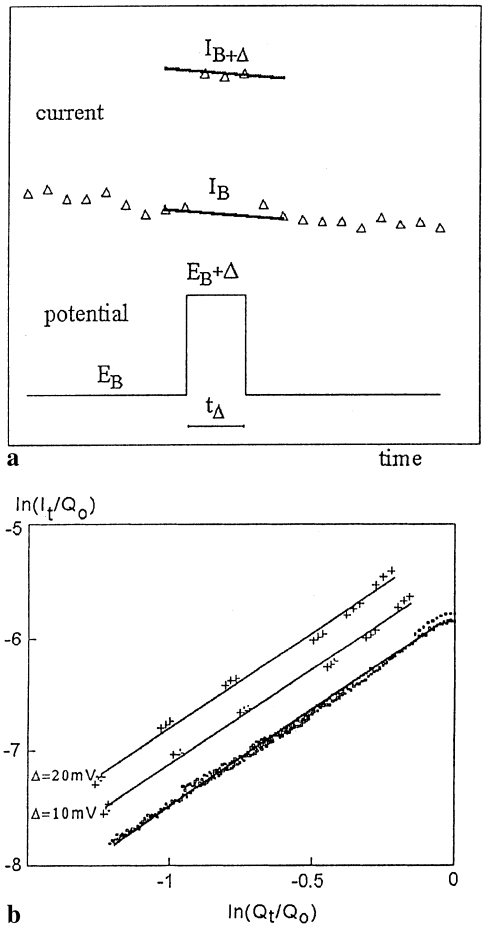

Fig. 2a, b The potential-jump method: **a** scheme of a single potential pulse, **b** a comparison of three runs with two-step pulses (sample $LaFe_{0.5}Cr_{0.5}O_3$, $E_B = 1.00$ V vs. SCE, pulses 10 and 20 mV, lines according to Eq. 8)

potential jump. When the obtained data were plotted in logarithmic variables $\ln(I_t/Q_0)$ vs $\ln(Q_t/Q_0)$, the points obtained during the potential jump lay on a curve parallel to that of the points obtained at E_B. The potential programme was finished by a 20- to 60-min application of a potential which was by 0.1–0.2 V more positive than the potential of the voltammetric peak (1 mV s^{-1}). This was sufficient to complete the dissolution. Complete dissolution is necessary to obtain Q_0 and the background currents at each utilised potential. The potential pulses can be repeated within a single measurement and hence a possible dependence of a_L on y can be determined.

The former potentiostatic method to obtain a is based on plotting $\ln[k(E)]$ vs E at low reaction rates (see Fig. 4 as an example). The obtained slopes, a, could be directly compared to a_L obtained at the same potential. The results obtained for substituted Cr perovskites are compared in Table 2 – there is no significant difference between both methods. Whereas the original potentiostatic procedure is suitable for reactions with relatively stable $f(y)$, the potential-jump method is applicable whenever the Faradaic component can be distinguished from the overall current. The potential-jump method also proved that the formal charge transfer coefficient is virtually independent of the fractional reaction y (see Figs. 2b and 3). Only a statistically non-significant decrease of a at $y > 50\%$ was found. The same is valid for other studied Cr oxides except the highly substituted ones (see below, $x > 0.5$). These results are a crucial proof of the validity of the separation of the charge transfer contribution to the electrochemical reactivity of microparticles [9].

Both methods to obtain formal charge transfer coefficients failed when the reaction rate at constant potential decreased much faster than could be expected for a surface reaction of solid particles. This reaction course was observed in the case of $LaCr_{1-x}Fe_xO_3$ and $Me(Cr_{1-x}Fe_x)_2O_4$ when x exceeds 0.5. In those cases, one can expect that the surface of dissolved particles is

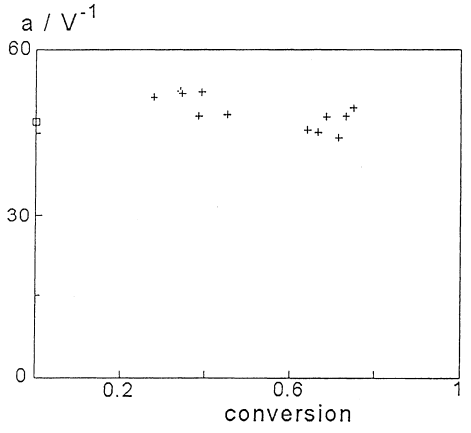

Fig. 3 A non-significant dependence of a formal charge transfer coefficient on the fractional reaction of perovskite $LaNi_{0.5}Cr_{0.5}O_3$. □ the simple potentistatic method (see Experimental), + the potential-jump method

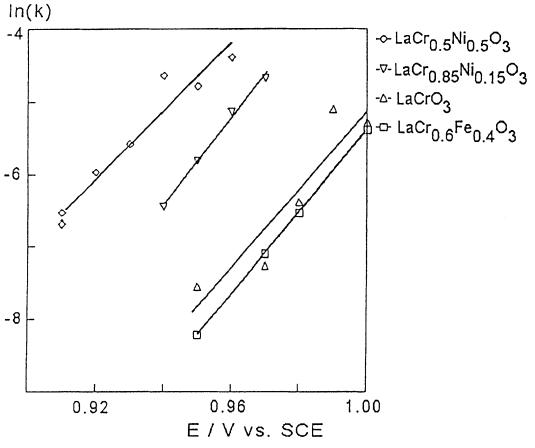

Fig. 4 $\ln(k)$ vs E for substituted Cr perovskites

continuously enriched in non-reactive components, as is common during the chemical dissolution of mixed oxides [1, 11, 23]. In the present case, the relative enrichment can occur in B-sublattices by leaking Cr and leaving a passive surface resembling that of $LaFeO_3$ or $MeFe_2O_4$.

The voltammetry of Cr oxides is similarly as phase-specific as the voltammetry of Fe oxides [12]. The peak potentials obtained at 1 mV s^{-1} in acid supporting electrolyte (see Table 3) increase in the following order:

$La(Cr,Ni)O_3, La(Cr,Co)O_3 < LaCrO_3 < La(Cr,Fe)O_3 < CrO_2 \ll Me^{II}Cr_2O_4 < \alpha\text{-}Cr_2O_3 < Me^{II}(Cr,Fe^{III})_2O_4$

where Me^{II} is Co, Fe, Ni or Zn. Voltammograms of the highly Fe-substituted spinels $CoFe_{1.5}Cr_{0.5}O_4$ and $ZnFe_{1.5}Cr_{0.5}O_4$ and the perovskite $LaCr_{0.25}Fe_{0.75}O_3$ exhibit non-separated peaks (denoted as "shoulders" in Table 3) beside a poorly defined wave. Regardless of the phase purity of the samples according to XRD, heterogeneity of the substitution cannot be excluded as it can occur in $\alpha\text{-}(Cr_{1-x}Fe_x)_2O_3$ [20]. We also observed that samples of $NiFeCrO_4$ obtained by various synthetic routes behaved differently. "Ceramic" synthesis from NiO, Fe_2O_3 and Cr_2O_3 (heating for 100 h at 1000 °C) yielded a solid that gave the mentioned shoulder, whereas the sample obtained by heating co-precipitated hydroxides (2 h at 1000 °C) was not electroactive. Both samples

Table 2 Formal charge transfer coefficients of substituted Cr perovskites as obtained by the potential-jump method and by a series of potentiostatic measurements. All given values have been obtained at potentials where a reaches its maximum value (at low potential)

Composition	a	
	Potential jumps	Potentiostatic method
$LaCrO_3$	52 (8)	47 (10)
$LaCr_{0.85}Ni_{0.15}O_3$	59 (3)	60 (3)
$LaCr_{0.5}Ni_{0.5}O_3$	55 (2)	52 (6)
$LaCr_{0.33}Ni_{0.67}O_3$	40 (8)	43
$LaCr_{0.6}Fe_{0.4}O_3$	50	49 (2)
$LaCr_{0.5}Fe_{0.5}O_3$	38 (3)	

Table 3 Potential of voltammetric peaks E_P, widths of peaks in the half of their height $E_{P/2}$ and a relative peak height I_P/Q_0 of Cr-containing oxides

Phase	Sample	E_P (V)	$E_{P/2}$ (V)	$10^3 \times I_P/Q_0$ (s^{-1})
Cr oxides	$(Cr_{0.99}Mg_{0.01})_2O_3$	1.34	0.13	7
	$(Cr_{0.95}Mg_{0.05})_2O_3$	1.335	0.13	7
	$(Cr_{0.9}Ti_{0.1})_2O_3$	1.445		
	Cr_2O_3	1.35	0.10	6
	Cr_2O_3	1.30	0.07	7
	CrO_2	1.16	0.08	11
Cr perovskites	$LaCrO_3$	1.02	0.07	12
	$LaCr_{0.95}Ni_{0.05}O_3$	1.02	0.05	18
	$LaCr_{0.85}Ni_{0.15}O_3$	0.99	0.06	15
	$LaCr_{0.7}Ni_{0.3}O_3$	0.96	0.07	13
	$LaCr_{0.5}Ni_{0.5}O_3$	0.98	0.07	13
	$LaCr_{0.5}Ni_{0.5}O_3$	0.99	0.05	16
	$LaCr_{0.33}Ni_{0.67}O_3$	1.01	0.09	11
	$LaCr_{0.5}Mn_{0.5}O_3$	0.95	0.08	12
	$LaCr_{0.5}Co_{0.5}O_3$	0.94	0.06	13
	$LaCr_{0.75}Fe_{0.25}O_3$	1.03	0.05	16
	$LaCr_{0.6}Fe_{0.4}O_3$	1.04	0.06	12
	$LaCr_{0.5}Fe_{0.5}O_3$	1.07	0.11	9
	$LaCr_{0.4}Fe_{0.6}O_3$		No peak	
	$LaCr_{0.25}Fe_{0.75}O_3$		Shoulder at 1.07	
Cr spinels	$CoCr_2O_4$	1.26	0.08	12
	$CoFe_{0.5}Cr_{1.5}O_4$	1.27	0.07	12
	$CoFe_{0.75}Cr_{1.25}O_4$	1.30	0.09	11
	$CoFeCrO_4$		No peak	
	$CoFe_{1.5}Cr_{0.5}O_4$		Shoulder at 1.26	
	$NiCr_2O_4$	1.29	0.09	9
	$NiFe_{0.5}Cr_{1.5}O_4$	1.36	0.07	13
	$NiFeCrO_4$		No peak	
	$ZnCr_2O_4$	1.22	0.08	11
	$ZnFe_{0.5}Cr_{1.5}O_4$	1.30	0.08	10
	$ZnFeCrO_4$	1.41		
	$ZnFe_{1.5}Cr_{0.5}O_4$		Shoulder at 1.30	

seemed to be a single-phase spinel according to XRD, but Mössbauer spectroscopy revealed several % of Fe in sextets resembling those of $NiFe_2O_4$ in the "ceramic" sample. It is probable that the voltammetric "shoulder" was caused by Cr-enriched domains or fractions of crystals.

The peak width can be characterised either by its half-width or by the peak current divided by the total charge of the peak. Both quantities are given in Table 3. There is a statistically significant dependence between $E_{P/2}$ and I_P/Q_0 because they are both affected mainly by a formal charge transfer coefficient and the number of exchanged electrons, and also by the kinetic characteristic γ (apparent reaction order). Unfortunately, the complexity of the corresponding equations excludes the derivation of mathematical formulae for these quantities. For example, the formal charge transfer coefficient a_L of each particular oxide decreases with the applied potential (see Fig. 5). This is known from experiments [8, 9, 12, 13] and it also follows from the surface-complexation model [9]. The interrelations between individual kinetic characteristics makes the mathematical processing of voltammetric peaks practically impossible. As a result, there are only qualitative conclusions for the peak width: it increases with the decreasing number of exchanged electrons, with the formal charge transfer coefficient, and with the increasing distribution of the particle sizes.

The value of a depends on the number of electrons exchanged in the electrochemical reaction. If an average value of α was around 0.6, as in the case of reductive dissolution of Fe oxides and hydroxy-oxides [8, 9, 12, 13], a should be expected around 25 for a one-electron exchange and around 50 for a two-electron exchange. Figure 5 would then show that the electrochemical dissolution of all Cr oxides is controlled by a two-electron reaction at low overpotential.

The actual dependence of a_L on E is determined by the reaction mechanism. For one-electron oxidative dissolution of a metal oxide based on the surface complexation model [9], the reaction rate depends on the potential according to Eq. 10

$$k(E) = \frac{k \exp(a(E - E_{\mathrm{eq}}))}{1 + k \exp(a(E - E_{\mathrm{eq}}))} k_{\mathrm{MAX}} \qquad (10)$$

where k and k_{MAX} are constants with the meaning of rate coefficients, and E_{eq} is a formal redox potential of the solid redox centre. Equation 9 produces a curve of a_L vs E with a single inflex at $E = E_{\mathrm{eq}}$. On the other hand, the dependence obtained for Cr oxides seems to possess two inflexes that can correspond to a pair of single-electron steps. We hence performed modelling resembling that described in [9] but involving two subsequent charge transfers according to Eqs. 2 and 4.

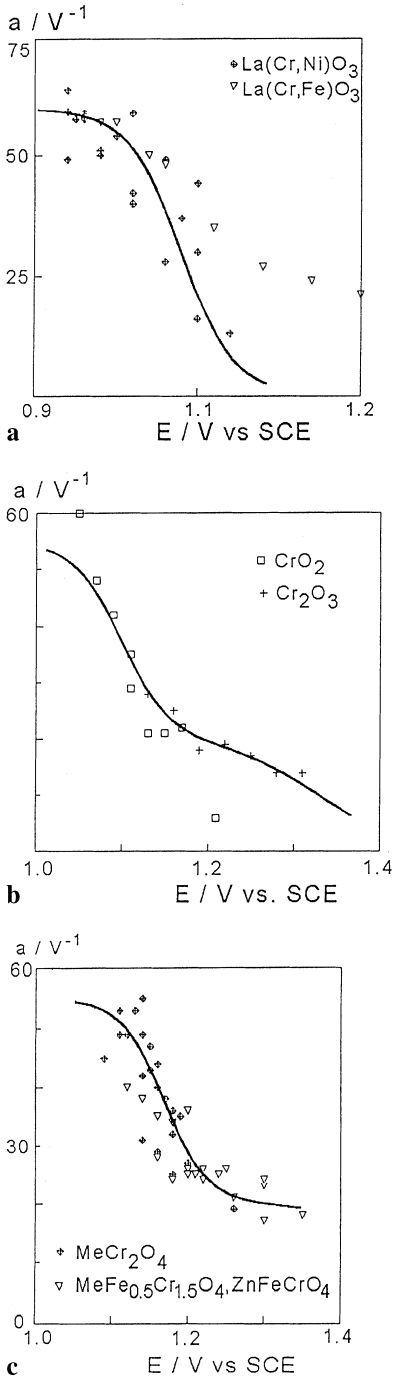

Fig. 5a–c a vs E for Cr oxides: **a** perovskites, **b** pure Cr oxides and **c** spinels. *Solid lines* are based on Eqs. 10 (**a**) or 16 (**b**, **c**)

Let us suppose that there are only $\{\equiv Cr^{III}\}$, $\{\equiv Cr^{IV}\}$ and $\{\equiv Cr^{V}\}$ in the Cr positions on the surface of dissolving Cr oxides

$$\{\equiv Cr^{III}\} + \{\equiv Cr^{IV}\} + \{\equiv Cr^{V}\} = \{\equiv Cr_{TOT}\} \quad (11)$$

Let us further suppose the redox cycling of individual Cr valences involves two reversible processes

$$\{\equiv Cr^{IV}\} = \exp[a_{34}(E - E_{34})]\{\equiv Cr^{III}\} \quad (12)$$

$$\{\equiv Cr^{V}\} = \exp[a_{45}(E - E_{45})]\{\equiv Cr^{IV}\} \quad (13)$$

where E_{34} and E_{45} are formal redox potentials of reactions according to Eqs. 2 and 4, respectively. The assumption of the redox reversibility is based on the observed fast equilibration of the current after the potential jumps. The reacting crystal surface fulfils the general requirements for electron hopping [21] due to short distances between neighbouring hopping centres $\{\equiv Cr^{III}\}$, $\{\equiv Cr^{IV}\}$ and $\{\equiv Cr^{V}\}$, and due to their similar coordination surroundings which are fixed by the crystal lattice. There is no indication of further oxidation of $\{\equiv Cr^{V}\}$ in the solid state. Furthermore, Cr^{VI} is tetrahedrally coordinated and so it cannot occur in the octahedral positions of low Cr oxides. The reaction of the solid should hence be completed by a dissolution

$$\{\equiv Cr^{V}\} \xrightarrow{k_d} CrO_4^{2-}(aq) \quad (14)$$

with the overall reaction rate J_d

$$J_d = k_d\{\equiv Cr^{V}\} \quad (15)$$

The solution of these equations is

$$J_d = \frac{k_d\{\equiv Cr_{TOT}\}}{1 + \exp[-a_{45}(E - E_{45})] + \exp[-a_{34}(E - E_{34})] \cdot \exp[-a_{45}(E - E_{45})]} \quad (16)$$

Equation 16 was used for the derivation of the dependence of a_L on E that is desired for processing the data obtained by the potential-jump method. This was also used to fit the obtained experimental data (see solid lines in Figs. 5b and 5c). Modelling shows that whenever the separation of E_{34} and E_{45} is of the order of several tenths of a volt, $a_L(E)$ possesses more than one inflex. The first inflex point of the studied oxides obtained by fitting are placed at 0.99 V for low-Ni-substituted $LaCrO_3$, 1.10 V for CrO_2 and Cr_2O_3, and 1.17 V for $Me(Cr_{1-x}Fe_x)_2O_4$ (all potentials are referred to SCE).

It is of theoretical importance to discuss the influence of electronic conductivity on the voltammetry of immobilised metal oxides. As is well known [21, 22], the Ni content in $LaCr_{1-x}Ni_xO_3$ markedly increases the solid phase conductivity without significant alteration of its crystal structure. In chemical terms, the formal valences of metals in substituted perovskites are $La(Cr^{III}_{1-2x}Cr^{IV}_xNi^{II}_x)$ at $x < 0.5$. Regardless of the continuously growing bulk conductivity with growing x, neither dissolution kinetics, i.e. the $f(y)$ function, nor a substantially changed with this substitution at $x \leq 0.5$. As follows from the example of Ni- and Fe-substituted $LaCrO_3$ (Fig. 5), the substitution affected mainly the rate coefficient at a given potential. On the other hand, the overall order of the growing potential of voltammetric peaks for all phases studied is obviously related to the decreasing bulk electronic conductivity of Cr oxides. Cr perovskites and CrO_2 are of substantially higher conductivity than α-Cr_2O_3 and chromites.

Discussion

General features of electrochemical dissolution of microcrystalline Cr oxides can be summarised as follows:

1. Complete dissolution can be performed within a single voltammetric measurement; the reaction at constant potential is most frequently described by general reaction order kinetics unless more than half of Cr is substituted by Fe.
2. Fast equilibration of the current after potential jumps (around 1 s at 0.01 V pulses) shows a remarkable rate of corresponding redox equilibration on the reacting surface regardless of a low electronic conductivity in the case of $MeCr_2O_4$, and α-Cr_2O_3.
3. The reaction rate-determining step is preceded by two subsequent one-electron reactions, as follows from the shape of the dependence of a_L on E.

Note that no particular attention was paid to significant differences in the bulk electronic conductivity of the Cr oxides studied, because it is supposed that they are all completely dissolved by the same mechanism. As a consequence, the experimental data processing is the same for all oxides studied although they include metallic conductors ($LaCr_{0.33}Ni_{0.67}O_3$, CrO_2) and semiconductors with higher ($LaCrO_3$) or lower (α-Cr_2O_3, $MeCr_2O_4$) conductivity. The same was also assumed for Fe oxides [8, 13]. The explanation is based on electron hopping between surface metal ions of the dissolving metal oxide accompanied by chemisorption of counterbalancing ions from the supporting electrolyte [9]. The same explanation has recently been given for the surprisingly fast spreading of charge over the surface of nonconducting crystals (an electron self-exchange) of organic complexes of Cr [24], alkylferrocene [25], a heteropolymolybdate salt [26] and azobenzene [27]. The process could hence be a very general reaction pathway in the voltammetry of immobilised poorly conducting microcrystals. Not bulk conductivity but rather the presence of appropriate hopping centres on the surface and a free access of counter-ions from the supporting electrolyte would hence determine the electrochemical activity of such solids. For example, the significant influence of substitution of electroactive metal ions in Cr or Fe oxides can be interpreted as dilution and separation of the remaining hopping centres $\{\equiv Cr^n\}$. When this dilution reaches a certain level, the reaction is no longer described by the kinetics of a surface reaction, and the corresponding voltammetric peak becomes wide and flat and finally virtually disappears. The critical degree of substitution is 10–15 mol% of Al in substituted α-FeOOH [13], and $\approx$50 mol% of Fe in substituted Cr spinels and perovskites. The most probable explanation why a high Ni content in $LaCr_{0.33}Ni_{0.66}O_3$ does not suppress the dissolution reaction is that the bulk electronic conductivity of this phase (above 1 Ω^{-1} cm^{-1} at $x > 0.5$ [22]) is sufficient for current transfer and hence the formation of the surface conducting layer is not a necessary prerequisite.

Conclusions

Voltammetry of immobilised microcrystalline Cr oxides is significantly affected by the phase composition and by the degree of Cr substitution. The presented potential-jump method permits obtaining formal charge transfer coefficients of electrochemical reactions of immobilised Cr oxides in a single experiment without the necessity to accept any specific kinetic model. The results obtained justify the separation of the potential-dependent rate coefficient $k(E)$ and the conversion-dependent function $f(y)$, which is of great importance for the general kinetics of the heterogeneous reactions of microcrystals [9]. Further indications were obtained that a surface conducting layer is formed on poorly conducting crystals that are subjected to a redox reaction in the solid phase.

References

1. Blesa MA, Morando PJ, Regazzoni AE (1994) Chemical dissolution of metal oxides. CRC Press, Boca Raton
2. Schwertmann U, Cornell RM (1996) The iron oxides. VCH, Weinheim
3. Segal MG, Williams WJ (1986) J Chem Soc Faraday Trans 82: 3245
4. Rodenas LG, Morando PJ, Blesa MA, Duhalde S, Saragovi C (1993) Can J Chem 71: 771
5. Rodenas LG, Chocrón M, Morando PJ, Blesa MA (1996) Can J Chem 74: 103
6. Scholz F, Lange B (1992) Trends Anal Chem 11: 359
7. Scholz F, Meyer B (1994) Chem Soc Rev 23: 341
8. Grygar T (1996) J Electroanal Chem 405: 117
9. Grygar T (1998) J Solid State Electrochem 2: 127
10. Mouhandess MT, Chassagneux F, Vittori O, Accary A, Reeves RM (1984) J Electroanal Chem 181: 93
11. White AF, Peterson ML, Hochella Jr MF (1994) Geochim Cosmochim Acta 58: 1859
12. Grygar T (1996) Coll Czech Chem Commun 61: 93
13. Grygar T (1997) J Solid State Electrochem 1: 77
14. Soustelle M, Pijolat M (1997) Solid State Ionics 95: 33
15. Bordère S, Rouquerol F, Rouquerol J, Estienne J, Floreancig A (1990) J Therm Anal 36: 1651
16. Málek J, Šesták J, Roquerol F, Roquerol J, Criado JM, Ortega A (1992) J Therm Anal 38: 71
17. Voleník K, Hanousek F, Strauch B (1981) Czech J Phys B 31: 86
18. Encinas Bachiller P, Tascón Garcia ML, Vázquez Barbado MD, Sánchez Batanero P (1997) J Electroanal Chem 424: 217
19. Lorenzo L, Encinas P, Tascón ML, Vázquez MD, de Francisco P, Sánchez Batanero P (1997) J Solid State Electrochem 1: 232
20. Musić S, Lenglet M, Popović S, Hannoyer B, Czakó-Nagy I, Ristiæ M, Balzar D, Gashi F (1996) J Mater Sci 31: 4067
21. Cox PA (1995) Transition metal oxides, an introduction to their electronic structure and properties, 2nd edn. Clarendon Press, Oxford
22. Höfer T, Schmidberger R (1994) J Electrochem Soc 141: 782

23. Kittaka S (1974) J Colloid Interface Sci 48: 334
24. Bond AM, Colton R, Daniels F, Fernando DR, Marken F, Nagaosa Y, Van Steveninck RFM, Walter JN (1993) J Am Chem Soc 115: 9556
25. Bond AM, Marken F (1994) J Electroanal Chem 372: 125
26. Bond AM, Cooper JB, Marken F, Way DM (1995) J Electroanal Chem 396: 407
27. Komorsky-Lovrić Š (1997) J Solid State Electrochem 1: 94